

## Microscopic structure of the Gamow-Teller resonance in $^{208}\text{Bi}$

H. Akimune<sup>a</sup>, I. Daito<sup>b</sup>, Y. Fujita<sup>c</sup>, M. Fujiwara<sup>b</sup>, M.B. Greenfield<sup>d</sup>, M.N. Harakeh<sup>e</sup>,  
T. Inomata<sup>f</sup>, J. Jänecke<sup>g</sup>, K. Katori<sup>f</sup>, S. Nakayama<sup>h</sup>, H. Sakai<sup>i</sup>, Y. Sakemi<sup>b</sup>,  
M. Tanaka<sup>j</sup>, and M. Yosoi<sup>a</sup>

<sup>a</sup> Department of Physics, Kyoto University, Kyoto 606, Japan

<sup>b</sup> Research Center for Nuclear Physics, Osaka University, Mihogaoka 10-1, Ibaraki,  
Osaka 567, Japan

<sup>c</sup> College of General Education, Osaka University, Toyonaka, Osaka 560, Japan

<sup>d</sup> Natural Sciences Division, International Christian University, Mitaka, Tokyo 181,  
Japan

<sup>e</sup> Kernfysisch Versneller Instituut, Zernikelaan 25, 9747 AA Groningen, The Netherlands.

<sup>f</sup> Department of Physics, Osaka University, Toyonaka, Osaka 560, Japan

<sup>g</sup> Department of Physics, University of Michigan, Ann Arbor, MI 48109-1120, U.S.A.

<sup>h</sup> College of General Education, Tokushima University, Tokushima, Japan

<sup>i</sup> Department of Physics, University of Tokyo, Bunkyo, Tokyo 113, Japan

<sup>j</sup> Kobe Tokiwa Jr. College, Nagata, Kobe 653, Japan

The  $^{208}\text{Pb}(^3\text{He},t)^{208}\text{Bi}$  reaction has been studied with the RCNP ring cyclotron at  $E(^3\text{He}) = 450$  MeV using the magnetic spectrometer Grand Raiden at  $\theta = 0^\circ$ . The Gamow-Teller resonance is strongly excited at this bombarding energy. Its microscopic structure has been investigated by measuring the direct proton decay to the neutron-hole states in  $^{207}\text{Pb}$ . The branching ratio for proton emission of a few % is much smaller than that for the decay of the isobaric analog state. The total width of the Gamow-Teller resonance as well as its total and partial escape widths have been determined. Several recent theoretical estimates for the escape width differ from the measured values by factors of  $\sim 2.5$ .

### 1. INTRODUCTION

Charge-exchange reactions play a very important role in the study of Gamow-Teller resonances (GTR) and other isovector giant resonances. In particular, the (p,n) reaction has successfully been used in the early observation of GTR [1-3]. Our knowledge of the systematics of the GT strength has increased significantly in recent years. This is based on the facts that the (p,n) reaction preferentially excites spin-flip  $\Delta L = 0$  states at bombarding energies  $> 100$  MeV, and furthermore that  $0^\circ$  cross sections are approximately proportional to  $B(\text{GT})$ . While the characteristics of GTR and the systematics of the GT strength including the dependence of the excitation energies, total widths, and the sum rule on mass number are quite well understood, very little is known about the microscopic structure of GTR.

The microscopic structure of GTR can be described as a coherent sum of particle-hole configurations where the proton particle and neutron hole occupy orbits which are spin-orbit partners. This structure can be investigated by measuring subsequent direct proton decay into single-neutron hole states of the respective daughter nucleus. No attempts have ever been made to do such studies with the  $(p,n\bar{p})$  reaction because of the low neutron detection efficiency and the limited energy resolution which precludes resolving decays into neighboring single-neutron hole states.

The  $(^3\text{He},t)$  reaction has several advantages which permit the investigation of direct proton decay. These include the efficiency of essentially 100% for detecting charged particles in a magnetic spectrometer at  $\theta = 0^\circ$  combined with the inherently superior energy resolution. Furthermore, the relatively wide acceptance angle combined with ray-tracing techniques permits the unique identification of  $\Delta L = 0$  as well as  $\Delta L \neq 0$  transitions from the angular dependence of the cross sections near  $\theta = 0^\circ$ . The  $(^3\text{He},t\bar{p})$  reaction has indeed been used at bombarding energies of typically 30 MeV/u to investigate the microscopic properties of isobaric analog states (IAS) which are strongly excited at these energies [4, 5]. An attempt has also been made to measure the proton decay from the GTR of  $^{208}\text{Bi}$  [4]. This attempt was not successful because the GTR was too weakly excited at the lower bombarding energy.

## 2. EXPERIMENT

The present report describes the first successful attempt to measure the proton decay of the GTR and to determine its microscopic structure. The experiment was performed at the Research Center for Nuclear Physics (RCNP) in Osaka. A 450 MeV  $^3\text{He}^{++}$  beam was extracted from the ring cyclotron [6], and transported onto a  $^{208}\text{Pb}$  target of 5.2 mg/cm<sup>2</sup> thickness and 99.86% isotopic enrichment. Tritons from the  $(^3\text{He},t)$  reaction were detected in the new spectrometer Grand Raiden [7] which has a K-value of 1400 MeV. The spectrometer was set near  $0^\circ$  and covered a solid angle of 1.6 msr. The  $^3\text{He}^{++}$  beam enters the spectrometer at  $0^\circ$ , and it is stopped inside the first dipole magnet. A test run with an empty target frame showed no background.

Singly-charged  $^3\text{He}^+$  particles are formed in the target with low yield by atomic charge-exchange processes. They arrive at the focal plane detector together with the ejectile tritons providing a good and convenient calibration standard for the beam energy and the scattering angle which is exactly  $0^\circ$ .

The ejectile tritons were detected with the focal-plane detection system [8] consisting of two 2-dimensional position-sensitive multi-wire drift chambers (MWDC) backed by two  $\Delta E$ -scintillation counters for particle identification. The MWDC allow the determination of the vertical and horizontal positions at the focal plane. The momentum, and thus the energy, of the scattered tritons can be deduced, and the horizontal and vertical scattering angles at the target can be reconstructed by ray-tracing techniques with uncertainties of about  $\pm 1.5$  mrad and  $\pm 5$  mrad, respectively. Because of the strongly forward-peaked angular distributions of the GTR and the IAS, software cuts on the deduced scattering angles have been applied in the off-line analysis to enhance the contribution of these two  $\Delta L=0$  transitions compared to transitions of higher multipolarity, which have minima in their angular distributions at  $0^\circ$ , and/or continuum background due to the quasi-free

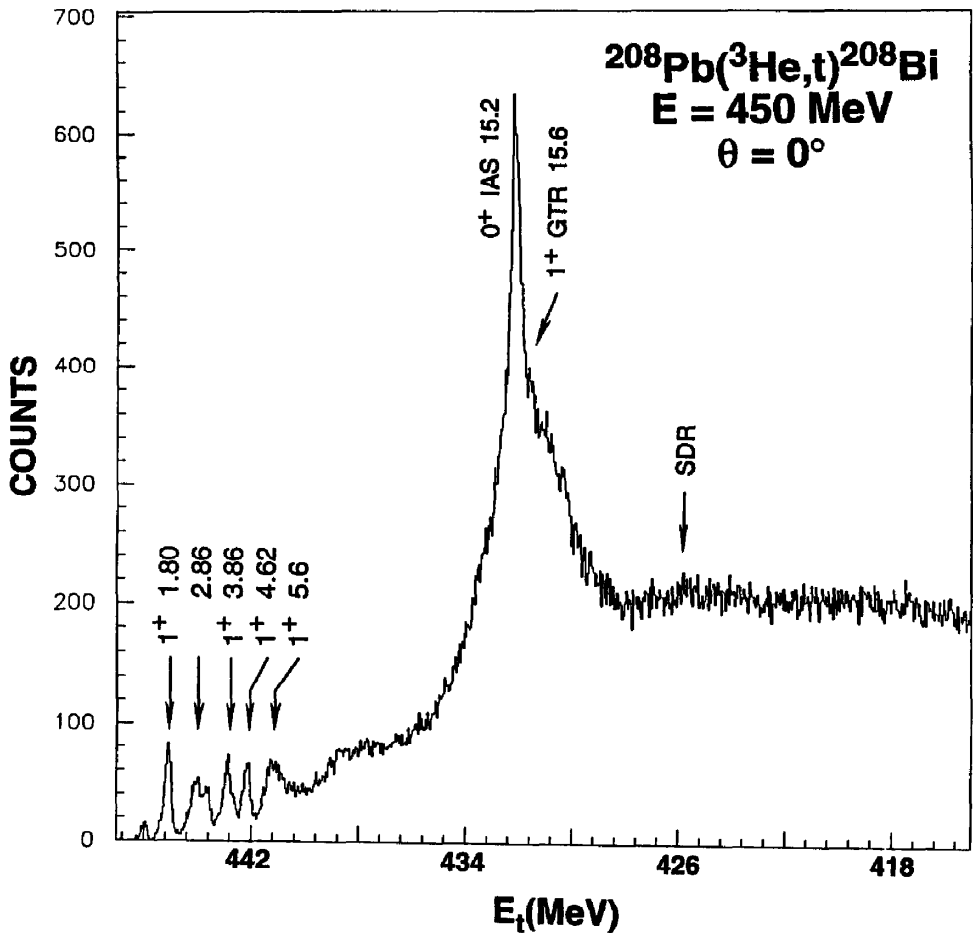


Fig. 1: Triton energy spectrum from the  $^{208}\text{Pb}(^3\text{He},t)^{208}\text{Bi}$  charge-exchange reaction at  $E(^3\text{He}) = 450 \text{ MeV}$  and  $\theta = 0^\circ$  measured with the magnetic spectrometer Grand Raiden. The spectrum was obtained by setting tight software gates centered near  $0^\circ$ . The spectrum enhances  $\Delta L=0$  transitions and hence the IAS and the GTR.

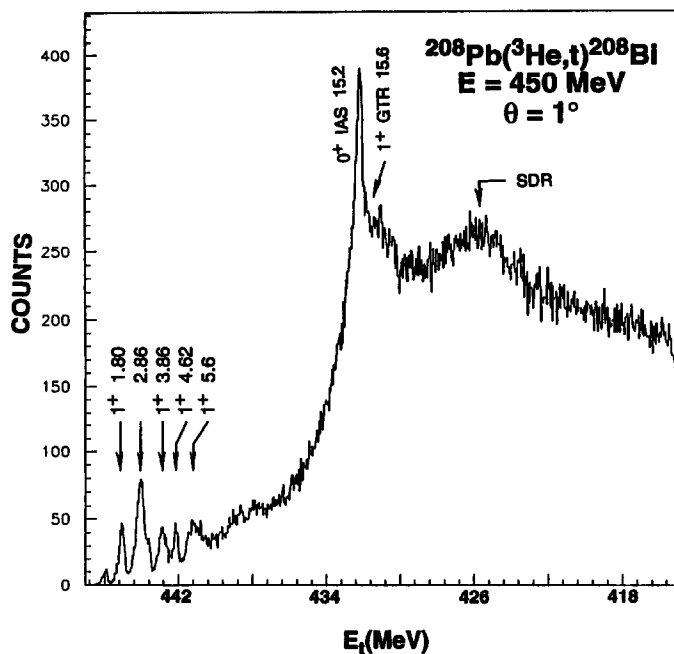


Fig. 2: Triton energy spectrum similar to Fig.1 but centered at  $\theta = 1^\circ$ . The spectrum enhances the spin dipole resonance (SDR).

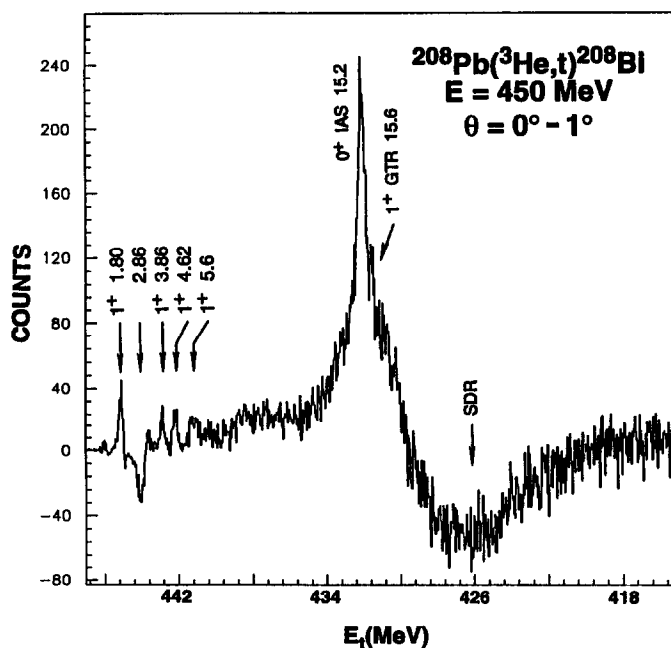


Fig. 3: Difference triton energy spectrum  $0^\circ - 1^\circ$  from the  $^{208}\text{Pb}(^3\text{He},t)^{208}\text{Bi}$  charge-exchange reaction. Transitions with  $\Delta L = 0$  are enhanced.

charge-exchange process, which has a rather flat angular distribution near  $0^\circ$ .

Figs. 1 and 2 display triton energy spectra for angles centered near  $0^\circ$

and  $1^\circ$ , respectively, with small solid angles of 0.07 msr. It is clear from these figures that the IAS and GTR as well as several low-lying  $1^+$  states are prominent in the  $0^\circ$  spectrum, whereas the spin dipole resonance with  $\Delta L = 1$  is enhanced in the  $1^\circ$  spectrum. These characteristics become even more apparent in the difference spectrum  $0^\circ - 1^\circ$  shown in Fig. 3.

Protons from the decay of the GTR were measured in coincidence with tritons detected at  $0^\circ$  in eight solid-state detectors (SSD) arranged in two rings containing 4 SSD's each. The detectors were set at distances of  $\sim 10$  cm from the target. The detectors in the outer and inner rings were positioned at  $\theta = 131.9^\circ$  and  $156.5^\circ$ , respectively, with azimuthal angles of  $\phi = 45^\circ, 135^\circ, 225^\circ$  and  $315^\circ$ . Each SSD had an area of  $490 \text{ mm}^2$ , but the detectors in both rings were collimated to cover solid angles of  $\Delta\Omega = 57.8$  and  $47.0$  msr, respectively. This yields a combined detection efficiency of 3.3%. Beam currents of up to 5 nA were used, and the count rate in the SSD's never exceeded 5 kHz.

Time-of-flight spectra were generated for all SSD's. These time spectra (not shown here) display several random peaks and one prompt peak with a prompt to random ratio of about 10. Two-dimensional spectra of proton-decay energy measured in the SSD's versus excitation energy in  $^{208}\text{Bi}$  were generated for prompt and random events. Fig. 4 displays a contour plot for the region of the GTR and IAS gated on scattering angles near  $\theta = 0^\circ$  and prompt events. The loci for decays into the g.s. and the low-lying neutron-hole states can clearly be observed. The excitation energies and configurations are listed in Table 1. The combined resolution of the triton and proton sum energy of about 400 keV was not sufficient to resolve the decay to the 1st and 2nd excited state of  $^{207}\text{Pb}$ . This can be seen in Fig. 5 which shows the projection of the loci on the excitation-energy axis of  $^{207}\text{Pb}$ . Only decays into the  $3p_{1/2}$ ,  $2f_{5/2}$ , and  $3p_{3/2}$  states are strong. Fig. 6, finally, displays a triton energy spectrum for prompt minus random coincidence events gated on angles near  $\theta = 0^\circ$  and proton decays to neutron-hole states in  $^{207}\text{Pb}$ . The relative contribution from the IAS compared to the GTR is much stronger than that seen in the singles spectrum of Fig. 1. This is due to the branching ratio for proton decay which is about 10 times stronger for the IAS. At excitation energies above the GTR it is observed that the spin-flip  $\Delta L = 1$  resonances still have finite cross sections near  $\theta = 0^\circ$ , and they also decay by proton emission to neutron-hole states in  $^{207}\text{Pb}$  [9].

### 3. RESULTS

The total width of the IAS, or the GTR, can be written as

$$\Gamma = \Gamma^\dagger + \Gamma^\ddagger, \quad (1)$$

where  $\Gamma^\ddagger$  is the spreading width and  $\Gamma^\dagger$  is the escape width. In the present case they are associated with neutron decay and direct proton decay to the neutron-hole states of  $^{207}\text{Pb}$ , respectively. The escape width can be written as

$$\Gamma^\dagger = \Gamma_p^\ddagger = \sum_i \Gamma_{p_i}^\ddagger, \quad (2)$$

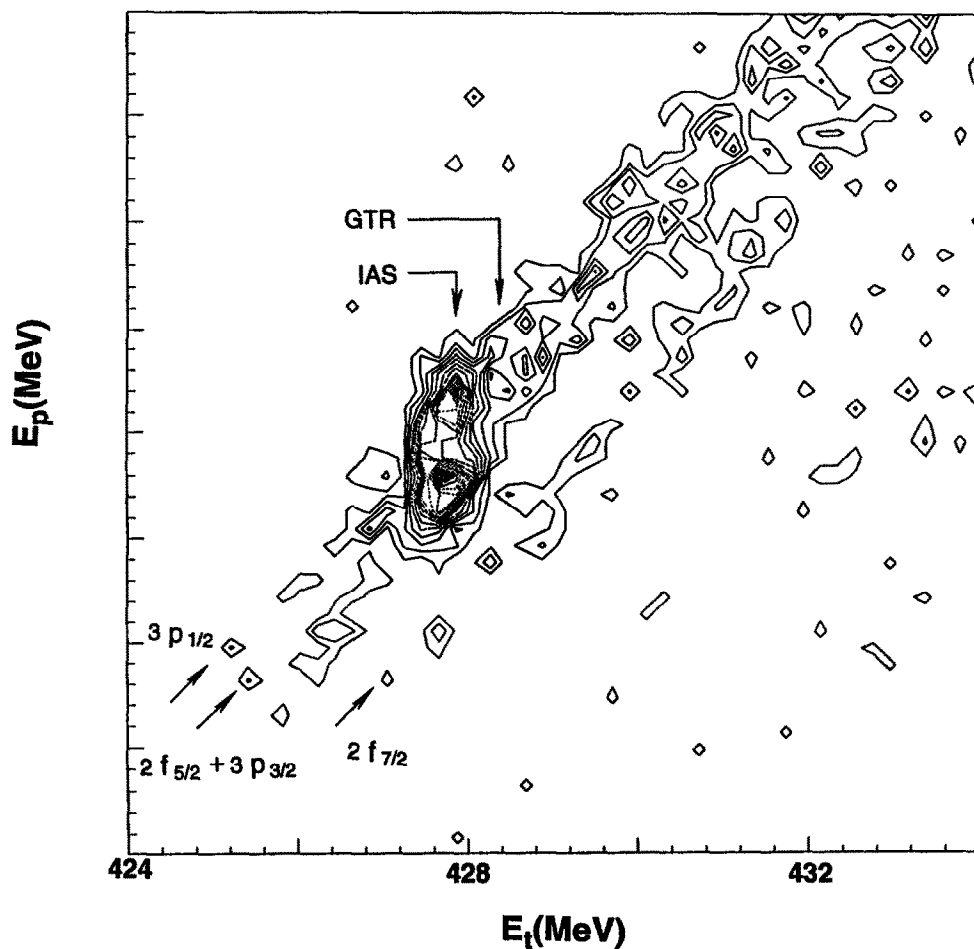


Fig. 4: Two-dimensional contour plot of proton decay energy versus triton energy [or  $E_x(^{208}\text{Bi})$ ] for the region of the IAS and GTR. The events are gated on prompt coincidences with scattering angles near  $\theta = 0^\circ$ . The uppermost line represents the locus for proton decay into the ground state of  $^{207}\text{Pb}$ .

Table 1

Theoretical and experimental partial and total escape widths,  $\Gamma_i^\dagger$  and  $\sum_i \Gamma_i^\dagger$ , in keV for the decay of the IAS (top) and GTR (bottom) in  $^{208}\text{Bi}$  into single-neutron hole states in  $^{207}\text{Pb}$ . The uncertainties of the experimental partial escape widths include only those of the measured partial branching ratios  $\Gamma_i^\dagger/\sum_i \Gamma_i^\dagger$ . The total widths  $\Gamma$  are  $231.6 \pm 6.0$  keV [15] for the IAS, and  $3750 \pm 250$  keV from the present work for the GTR.

neutron-hole states in $^{207}\text{Pb}$	$E_x(\text{keV})$ (a)	theor (b)	theor (b)	theor (c)	theor (d)	exp (e)	exp (h)
$3p_{1/2}^{-1}$	0	15.6	53.1	47.8	39	$51.9 \pm 1.6$	$51.4 \pm 5.6$
$2f_{5/2}^{-1}$	570	0.5	16.3	12.5	17	$26.4 \pm 2.0$	incl. in $p_{3/2}$
$3p_{3/2}^{-1}$	898	18.2	45.6	43.2	49	$64.7 \pm 3.4$	$79.4 \pm 9.4$
$1i_{13/2}^{-1}$	1633	0.6	2.0	0.5	0.11		
$2f_{7/2}^{-1}$	2340	0.2	0.4	0.1	4.4	$4.2 \pm 0.6$	$3.5 \pm 1.6$
$1h_{9/2}^{-1}$	3413	0.0	0.1	0.1	0.01		
total		35.1	117.5	104.2	110	$147.2 \pm 4.3$	$134.3 \pm 35.6$
	(a)	(b)	(b)	(f)		(g)	(h)
$3p_{1/2}^{-1}$	0	123.7	114.1	33		$570 \pm 70$	$48.9 \pm 9.3$
$2f_{5/2}^{-1}$	570	192.8	108.7	18		incl. in $p_{3/2}$	incl. in $p_{1/2}$
$3p_{3/2}^{-1}$	898	239.5	181.1	21		$1130 \pm 300$	$84.9 \pm 13.1$
$1i_{13/2}^{-1}$	1633	7.1	6.3	0.04		$1780 \pm 500$	$6.9 \pm 7.7$
$2f_{7/2}^{-1}$	2340	16.6	4.8	0.02		$850 \pm 300$	$13.1 \pm 6.2$
$1h_{9/2}^{-1}$	3413	7.9	2.9	0.26			
total		587.6	421.9	72		$\sim 4330$	$153.8 \pm 57.2$

- a) Nucl. Data Sheet.
- b) Ref. [11].
- c) Ref. [13].
- d) Ref. [14].
- e) Ref. [10] and references therein.
- f) Ref. [12].
- g) Ref. [4].
- h) Present experimental results.

where  $\Gamma_{p_i}^\uparrow$  is the partial proton escape width associated with decay into the  $i$ th neutron-hole state of  $^{207}\text{Pb}$ . The ratio of  $\Gamma^\uparrow$  to the total width  $\Gamma$  can be obtained for GTR and IAS from the ratios of the coincidence to single yields (Figs. 1 and 6) integrated over the respective excitation energies and corrected for the solid angle of the proton detectors. The decays of the GTR and IAS are assumed to be isotropic.

The partial proton escape widths obtained from the analysis of the data for the IAS and GTR are given in Table 1. Also shown are theoretical predictions and other experimental results. As noted above, the decays into the 1st and 2nd excited state of  $^{207}\text{Pb}$  could not be resolved.

The widths obtained for the IAS are in very good agreement with the experimental widths determined earlier [10]. The theoretical predictions confirm the observed dominance of the decays into the  $3p_{1/2}$ ,  $2f_{5/2}$ , and  $3p_{3/2}$  states, and the general agreement with the data is quite good.

As noted above, an earlier attempt to measure the partial decay width for the GTR [4] was unsuccessful due to the low bombarding energy and yielded values which were much too big. The new data confirm the theoretically predicted dominance of the decays into the three lowest single-neutron hole states. Also, two of the three calculations predict significant decay into the  $2f_{7/2}$  state which was observed. However, the theoretically predicted total escape widths [11, 12] agree only moderately well with the observed widths. The theoretical results of Van Giai et al. [11] performed within the framework of a self-consistent microscopic theory appear a factor of about three too big, and those of Muraviev and Urin [12] obtained in the RPA framework appear a factor of about two too small. It is not the purpose of this work to present a critical assessment of the theoretical approaches taken by these authors.

In conclusion, the proton decay of the GTR in  $^{208}\text{Bi}$  has been measured successfully for the first time yielding the total and partial escape widths for decays into single-neutron hole states in  $^{207}\text{Pb}$ . The branching ratio for proton emission of  $4.1 \pm 1.5\%$  is very small. Only moderate agreement has been achieved with theoretical predictions. The new data will help to improve the understanding of the microscopic structure of this basic collective mode of excitation and may contribute to a future understanding of the quenching of the Gamow-Teller strength.

The authors acknowledge the great help of the RCNP cyclotron staff and operators in the running of this experiment. Two of the authors (M.N.H. and J.J.) acknowledge the JSPS fellowship allowing them to participate in this experiment.



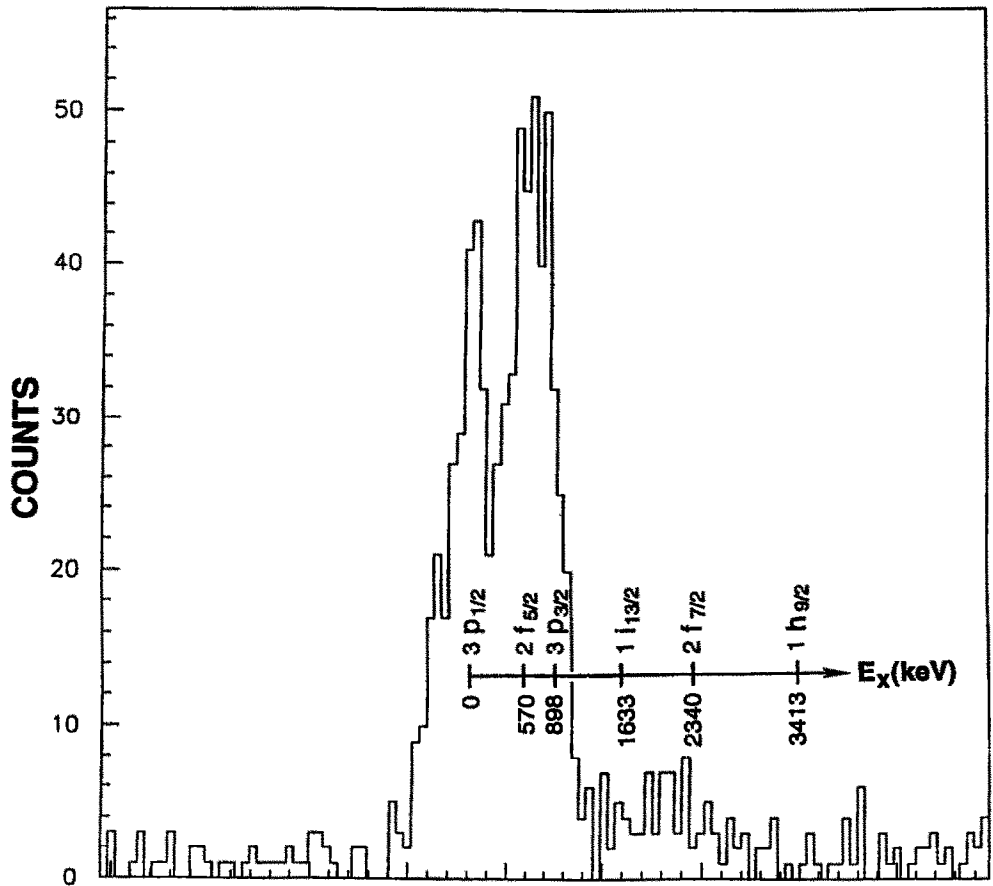


Fig. 5: Spectrum of decay protons into final neutron-hole states in  $^{207}\text{Pb}$  obtained from projecting events shown in Fig. 4 for the region of the GTR and IAS.

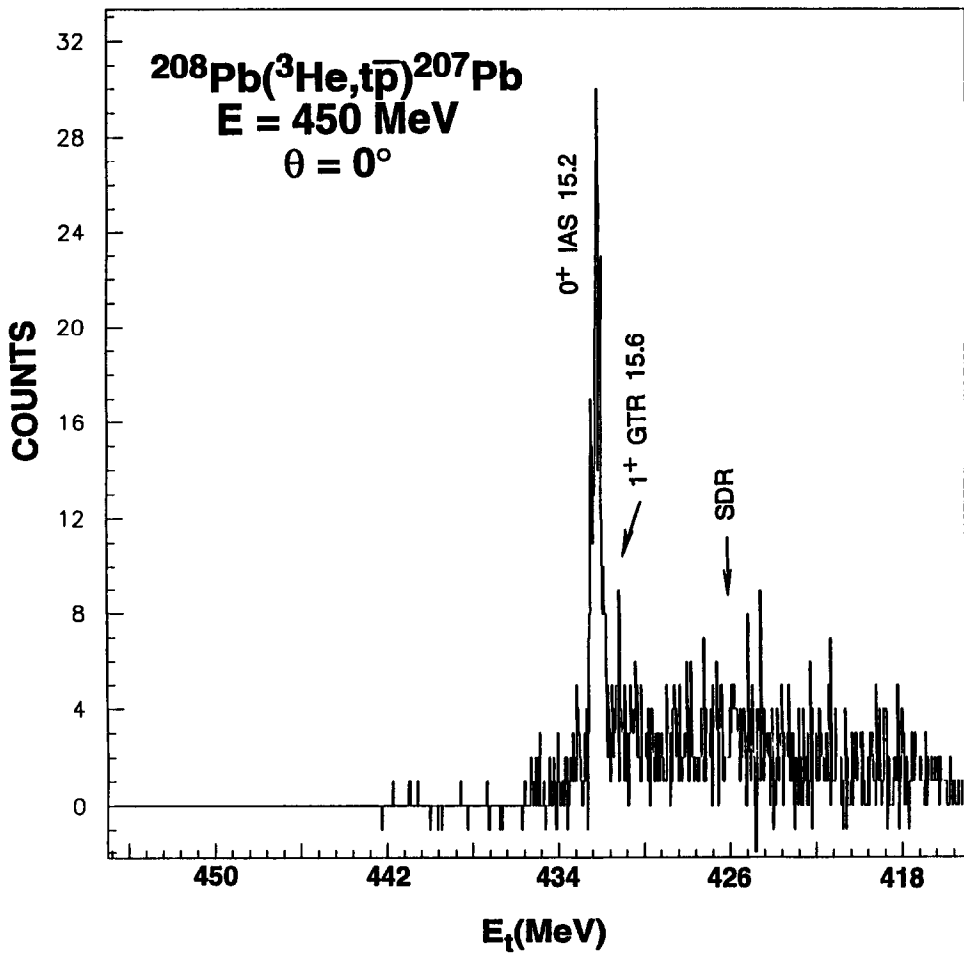


Fig. 6: Triton energy spectrum from  $^{208}\text{Pb}(^3\text{He},t\bar{p})^{207}\text{Pb}$  gated on events near  $\theta = 0^\circ$  and proton decays (prompt minus random) into ground and low-lying neutron-hole states in  $^{207}\text{Pb}$ .

## REFERENCES

1. D.E. Bainum et al., Phys. Rev. Lett. **44** (1980) 1751.
2. C.D. Goodman et al., Phys. Rev. Lett. **44** (1980) 1755 .
3. D.J. Horen et al., Phys. Lett. **B95** (1980) 27.
4. C. Gaarde et al., Phys. Rev. Lett. **46** (1981) 902.
5. H.J. Hofmann et al., Nucl. Phys. **A433** (1985) 181, and references therein.
6. I. Miura et al., RCNP Ann. Rep. (1991) 149.
7. M. Fujiwara et al., Nucl. Instr. Meth. Nucl. Res. **A**, to be published.
8. T. Noro et al., RCNP Ann. Rep. (1991) 177.
9. H. Akimune et al., to be published.
10. S.Y. van der Werf, M.N. Harakeh and E.N.M. Quint, Phys. Lett. **B216**, (1989) 15, and references therein.
11. N. Van Giai et al., Phys. Lett. **B233** (1989) 1.
12. S.E. Muraviev and M.G. Urin, Nucl. Phys. **A** to be published; private communication.
13. S. Yoshida and S. Adachi, Z. Physik **A325** (1986) 441.
14. V.G. Guba and M.G. Urin, Nucl. Phys. **A460** (1986) 222.
15. R. Meltzer, P. von Brentano and H. Paetz gen. Schiek, Nucl. Phys. **A432** (1985) 363.